Life Prediction and Classification of Fault-Modes in Solid State Lamps Using Bayesian Probabilistic Models

Pradeep Lall, Junchao Wei, Peter Sakalaukus
Auburn University
Department of Mechanical Engineering and
NSF CAVE3 Electronics Research Center
Auburn, AL 36849
Tele:(334)844-3424
E-mail:lall@auburn.edu

***Abstract* — A new method has been developed for assessment of the onset of degradation in solid state luminaires to classify failure mechanisms by using metrics beyond lumen degradation that are currently used for identification of failure. Luminous Flux output, Correlated Color Temperature Data on Philips LED Lamps has been gathered under 85°C/85%RH till lamp failure. The acquired data has been used in conjunction with Bayesian Probabilistic Models to identify luminaires with onset of degradation much prior to failure through identification of decision boundaries between lamps with accrued damage and lamps beyond the failure threshold in the feature space. In addition luminaires with different failure modes have been classified separately from healthy pristine luminaires. It is expected that, the new test technique will allow the development of failure distributions without testing till L70 life for the manifestation of failure.**

Keywords—Solid State Lighting, Life Prediction, Luminous Flux, Correlated Color Temperature, Bayesian Probabilistic Models.

I. INTRODUCTION

The lighting industry is undergoing a change from the incandescent lamps and compact fluorescent lamps (CFL) to light emitting diodes (LED). Mercury widely used in CFLs has the potential of contaminating large amounts of drinking water to beyond drinkable levels even in trace amounts. Transition to LEDs can impact energy efficiency tremendously because nearly 17% of the annual energy consumption is used for lighting [US EIA 2012]. LEDs are being used in a wide variety of applications including automotive lighting, LED displays, street and home lighting. Traditional methods of failure-detection often used for identification of failure in incandescent lamps may not be applicable to LEDs. Traditional light sources "burn out" at end-of-life. For an incandescent bulb, the lamp life is defined by B50 life or the time by which 50% of the population will fail. However, the LEDs have no filament to "burn". The LEDs continually degrade and the light output decreases eventually below useful levels causing failure. LED failure is characterized by L70 life or 70% degradation of the lumen output [IES LM-80-08; IES TM-21-11]. Currently, it is not possible to qualify SSL lifetime of 10-years and beyond often necessary of high reliability applications, primarily because of lack of accelerated test techniques and comprehensive life prediction models. SSL comprises of several length scales with different failure modes at each level. Interactions between optics, drive electronics, controls and thermal design. Accelerated testing for one sub-system may be too harsh for another sub-system. New methods are needed for predicting SSL reliability for new and unknown failure modes. Presently, there is scarcity of life distributions for LEDs and SSLs which are needed to assess the promised lifetimes. Several cities are experimenting with large scale deployment of luminaries. In order to keep high availability of the system, it is essential that the onset of damage in form of color shift, luminous output degradation, and change in CCT be detected early.

Previous researchers have studied the failure modes of luminaires. Junction temperature of a luminaire plays a substantial role on its lifetime. The degradation rate of the plastic encapsulation material (PEM) on the diode is predominately affected by junction temperature causing the attenuation of the light output [Narendran 2004, Baillot 2010]. Excessive temperatures inside the LED package or the ingress of moisture can produce thermal-mechanical and hydro-mechanical stresses between the various material layers of LED packages causing delamination [Lumileds 2006, Luo 2010]. Elevated temperatures and humidity can produce delamination between the die and silicone encapsulant [Lumileds 2006] and between the encapsulant and packaging lead frame [Luo 2010]. The stresses can also produce a hairline cracks known as lens cracking, which occurs due to thermal expansion at various operating temperatures [Lumileds 2006, Hsu 2008], as well as when a long-term exposure to moisture [Hewlett Packard 1997]. Ahn [2014] has examined the effect of

LED lighting on the heat loads in office buildings and showed that the energy consumption related to cooling of the building reduced in the neighborhood of 11-percent. Chan [2011] examined the accelerated life test of high power white light emitting diodes under exposure to temperature and humidity and found the degradation mechanisms of optical power reduction and degradation of blue wavelengths of emitted light due to bubbling and discoloration of silicone encapsulating material of the package. Choi [2014] studied the correlation between reliability and pH changes of phosphors for white light emitting diodes and showed that the reactivity of phosphor with water depended on the host material and could be identified through pH measurement. Fu [2012] investigated the dynamic color change mechanisms in high power light emitting diodes and found yellowed reflector and damaged silicone caused color shift. Jang [2014] studied the optimum design of radial heat sink for high-power LED lighting applications and found that pin-fin arrays with tallest pin heights in the outermost array exhibited the best performance. Meneghini [2012] studied the effect of DC and pulse wave modulation on the reliability in GaN light emitting diodes and found that in both cases higher stress levels caused higher degradation with PWM exhibiting a higher values of degradation. Yang [2010] investigated the failure and degradation mechanisms of high-power white light emitting diodes under exposure to high temperature and electrical currents and found that degradation rates of luminous flux increased with electrical and thermal stress. High electric stress induced surface and bulk defects in LED chip during short term aging.

In this paper, wet high temperature operating life environmental conditions of 85℃ and 85%RH have been used to understand the reliability of solid state luminaires. SSL failure is quantified by the deterioration of luminous flux output and correlated color temperature (CCT) with respect to the time during accelerated testing. The Illuminating Engineering Society test standards LM-80-08 and IES TM-21-11 define the lifetime of an LED for lighting as the degradation to 70-percent of the original luminous flux output at room temperature [IES LM-80-08; IES TM-21-11]. Bayesian generative models have been used for classification of damaged assemblies and Bayesian regression models have been used to model the damage progression in solid state luminaires. The luminous flux, CCT, and the color shift have been used as input variables for identification of the onset of damage and separation of the healthy SSLs from those with significant accrued damage. Discriminant functions have been used to identify the class boundaries and classify SSLs significantly prior to the development of complete failure distributions. The models have been used to estimate the remaining useful life for each sample under test and the model predictions validated versus experimental data. It is expected that, the new test technique will allow early identification of failure distributions.

II. TEST VEHICLE

One of the original off-the-shelf 60W LED Lamps has been used as the test vehicle (Figure 1). The lamp has a total of 9 LUXEON Royal-Blue LEDs which are divided into three systematic lamp housings with a yellow cerium doped yttrium aluminium garnet phosphor shell.

Figure 1 Ambient LED 60W Lamp

The lamp produces white light through the color mixing of the blue LEDs and the yellow phosphor. The luminaires have been subjected to temperature-humidity at 85℃/85RH in an accelerated test chamber. The luminaires were non-functional during the accelerated test and placed upright inside a lamp holder to prevent movement inside the test chamber. Each of the lamps were extracted on a weekly basis to exam the spectral data for luminous maintenance, chromaticity shift, and correlated color temperature. All of the lamps in the test set were aged in the temperature-humidity condition for a total duration of 2537 hours.

III. EXPERIMENTAL SET-UP

The LED lamp measurement has been accomplished using an integrating sphere. Typically, the lamp measurement system contains parts: (1) Light Emitting Device. (2) Light Gathering System. (3) Light Transmitting System. (4) Light Analyzing System. The light emitting device provides the AC voltage power connection to the LED lamp that is producing continuous measureable light. The Light Gathering System, in this case the integrating sphere redistributes and collects the entire light beam emitting from the LED lamp. The integrating sphere is an optical component that uniformly scatters the light, which has a special coating on its surface of inside sphere. With a small exit ports on the side of sphere, the LED lights can be transmitted through the cosine diffuser, which is a detector, filtering and transferring the distributed light to the cable optical fiber. Then, the light is carried into the Labsphere 'USB4000' Spectrometer. Data on the Lumen Flux and CCT is collected using SpecraSuite Software. The total spectral radiant flux, $\Phi_{test}(\lambda)$, of the LED lamps under test was obtained by comparison of the total spectral radiant flux of the test lamp, $\Phi_{TEST}(\lambda)$, to the total spectral radiant flux of a reference standard, $\Phi_{REF}(\lambda)$. The following equation was used to compute the total spectral radiant flux:

$$\Phi_{TEST}(\lambda) = \Phi_{REF}(\lambda) * \frac{y_{TEST}(\lambda)}{y_{REF}(\lambda)} * \frac{1}{a(\lambda)} \quad (1)$$

Where $y_{TEST}(\lambda)$ is the are the spectrometer readings for the lamp under test, $y_{REF}(\lambda)$ is the spectrometer readings for the reference-lamp, respectively, and $a(\lambda)$ is the self-absorption factor measured using an auxiliary lamp as

described in LM-79. From the measured total spectral radiant flux $\Phi_{TEST}(\lambda)$ [W/nm], the total luminous flux $\Phi_{TEST}(\lambda)$[lm] is obtained by

$$\Phi_{TEST} = K_m \int_{\lambda} \Phi_{TEST}(\lambda) * V(\lambda) d(\lambda)$$
$$K_m = 683 lm/W \quad (2)$$

Where $V(\lambda)$ is the photopic sensitivity as a function of the wavelength. Self-absorption is the effect, in which the response of the sphere system is affected due to the absorption of light by the lamp itself in the sphere. Errors can also occur if the size and shape of the test light source are significantly different from those of the standard light source. The self-absorption factor is given by,

$$a(\lambda) = \frac{y_{aux,TEST}(\lambda)}{y_{aux,REF}(\lambda)} \quad (3)$$

Where $y_{aux,TEST}(\lambda)$ is the spectrometer readings for the auxiliary lamp with the LED lamp in the sphere, and $y_{aux,REF}(\lambda)$ is the spectrometer readings for the auxiliary lamp with the reference standard in the sphere.

IV. Decay Rate And Failure Threshold

The decay rate of the luminous flux and the correlated color temperature in the LED lamps and the LUXEON LEDs inside the LED lamps has been calculated from the exponential model. The degradation model for lumen maintenance and correlated color temperature has been selected because the degradation of light emitting diodes has been modeled using the exponential model in IES TM-21-11 for life prediction of light emitting diodes in operation. Furthermore, the authors have used the exponential model for L70 life prediction in conjunction with Kalman Filter and Extended Kalman Filter [Lall 2013]

$$\Phi = \beta \cdot e^{\alpha \cdot t} \quad (4)$$

Where, β is the pre-decay factor, α is the decay rate, t is the test time, and Φ is either the luminous flux output or the correlated color temperature depending on the decay rate being calculated. The decay rate is a function of temperature and represented by:

$$\alpha = A \cdot e^{-\left(\frac{E_A}{k_B \cdot T}\right)} \quad (5)$$

Where T is the temperature in kelvin, K_B is the Boltzmann constant, and E_A is the activation energy. The Method of Least Square (LS) has been used to compute the decay rate for both CCT and Lumen Maintenance. The data for the LED lamps has been taken from accelerated test data under 85°C/85%RH. The LUXEON LEDs data from [DR05-1-LM80; Philips 2012] is under conditions of 55°C/65%RH at 1A. The two test conditions used for calculation of the activation energy include 55°C and 85°C. Measured values of both the luminous flux output and the correlated color temperature have been normalized with respect to the measured value at time zero. LED lamp data shows the degradation of CCT to 96% from the initial value of 100% after 2500 hours. Similarly, the Lumen Maintenance shows degradation to 68% after 2000 hours of accelerating test.

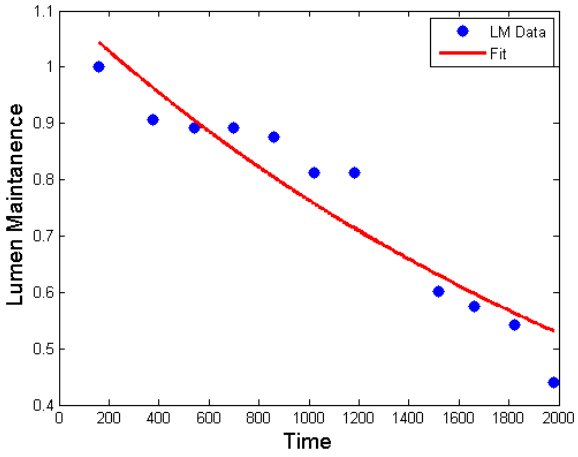

Figure 2: Lumen Maintenance Evolution for the LED Lamp in 85°C/85RH

Typically, L70 (70% Lumen Maintenance) life has been treated as the failure threshold for the luminous flux output of the solid state luminaire. Further, the 7-step MacAdam ellipse states that the target 'Duv' and its tolerance is ±0.006, and the corresponding target CCT and tolerance is 3000±175K for a nominal 3000K lamp [ANSI C78.377-2008 Specification]. One can therefore conclude that variation of CCT of greater than 94.17% of the original CCT values are deemed as unacceptable. The 94.17% value for a 3000K lamp is 2825K for the LED lamp. The lumen decay is more significant than the CCT decay. For the purpose of computing the remaining useful life of the luminaire and LEDs, the degradation of lumen maintenance was used. Figure 2 and Figure 3 show the decay rates for luminous flux output and correlated color temperature.

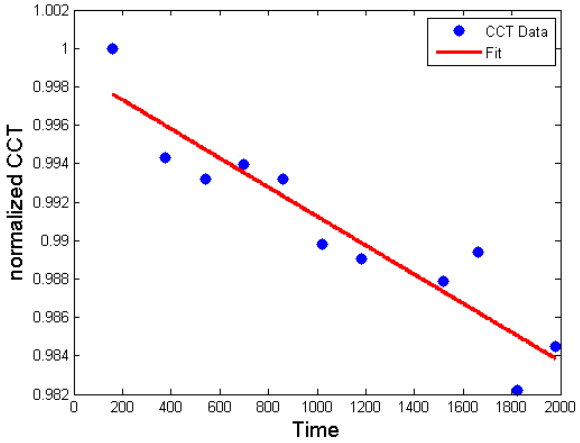

Figure 3: Correlated Color Temperature Evolution for the LED Lamp in 85°C/85RH

V. Decay Rate Distribution

Decay rate has been computed based on testing of LED Lamps. The testing length of time is 2536.85 hours. The mean value of L70 hours is 1673.3 hours. Figure 4 and Figure 5 show the lumen degradation and Correlated Color Temperature (CCT) versus time. We can see that there is distinct lumen degradation throughout the testing history. The CCT has dropped 2.49% compared to the pristine value at the end of testing for the L-prize lamp. It could have combined two types of degradation pattern in the

lumen. One is decelerating decay, and the other is accelerating decay. We will evaluate this behavior using one cubic polynomial model, which could better present this degradation curve than parabolic model.

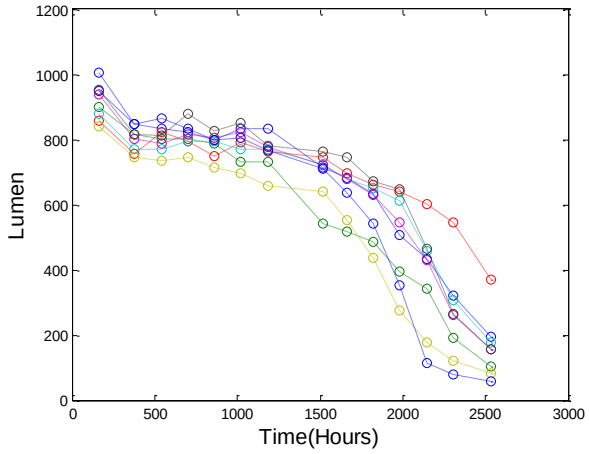

Figure 4: Lamp Lumen Depreciation in History

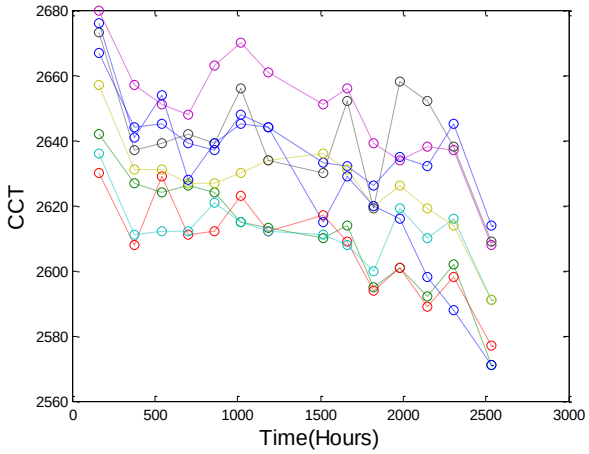

Figure 5: Lamp lamp CCT depreciation in History

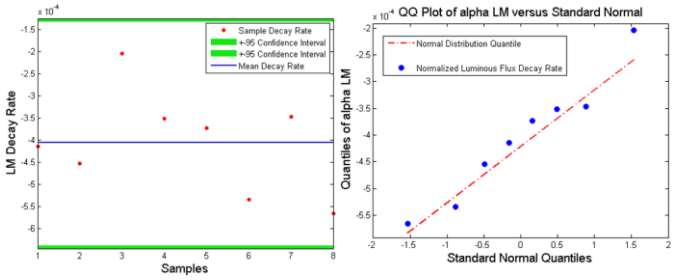

Figure 6: Fitted LM Decay Rate Distribution and QQ plot.

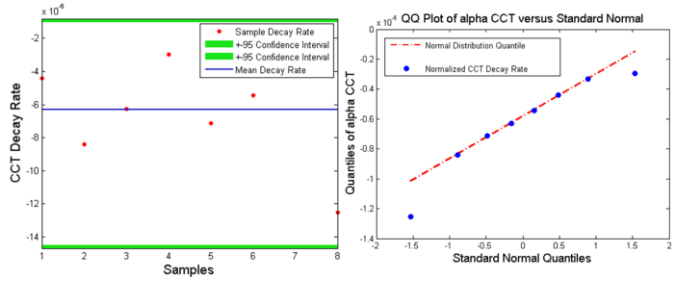

Figure 7: Fitted CCT Decay Rate Distribution and QQ plot

Similarly, the LM and CCT decay rate distribution for the L-prize is also normally distributed. Therefore, both the mean value and variance can be represented as the main decay character. The mean decay rate of normalized luminous flux output for the LUXEON LEDs has been calculated to be -5.14e-06 per hours, and mean decay rate of the normalized CCT for the LUXEON LEDs has been calculated to be -1.28e-06 per hours. Normality of the luminous flux output and the correlated color temperature distributions has been checked using the QQ-plot (Figure 6 and Figure 7). The red line shows the quantile of normal distribution, the blue dots show the decay rate of normalized luminous flux output and correlated color temperature data. Analysis results indicate that the data is normally distributed with only two or three outliers.

The decay rates for the normalized luminous flux output and the correlated color temperature of the lamp has been similarly computed to be -4.05e-04 per hours, and -6.30e-06 per hour respectively. The Arrhenius model has been used to calculate the activation energy for the normalized luminous flux output and the normalized correlated color temperature. The computed activation energy has been used to evaluate the effect of temperature on the luminous flux output and the correlated color temperature.

$$E_A = -\left(\frac{\ln \frac{\alpha_1}{\alpha_2}}{\left(\frac{1}{T_1} - \frac{1}{T_2} \right) \cdot K_B} \right) \quad (6)$$

The activation energy for the normalized lumen degradation is 1.47 eV and the activation energy for the normalized correlated color temperature is 0.53 eV. The failure threshold for the normalized luminous flux and the normalized correlated color temperature was identified by computing the 95% confidence bounds. Data that fell below the failure threshold at any time during the life test was deemed as a failure. Remaining useful life predictions were done for samples that did not fall below the failure threshold. The failure criterion is the curve of the maximum normalized decay rate, which will envelop all the degradation lines in the tested sample-set. For the LUXEON LEDs, the maximum decay rate ($\alpha_{max,LM}$) for the normalized luminous flux output is -6.77e-06 hour^{-1} and maximum decay rate ($\alpha_{max,CCT}$) for the normalized CCT is -2.8e-06 hour^{-1}. The 95% Confidence Interval for the maximum decay rate has been used to compute the highest possible decay rate, i.e. the lower boundary, for formulating the failure criterion. The maximum degradation rate has been used because it will encompass the worst possible parts in the population and prevent the labelling of parts within the ±1.96σ bounds as failures. If the mean lumen degradation and correlated color temperature had been used – then parts lower than the mean would have been labeled as a false-positives

$$\alpha_{LM}^{failure} = \alpha_{max,LM} - 1.96 \frac{\sigma}{\sqrt{N}} \quad (7)$$

$$= -7.04 \times 10^{-6} \text{ hour}^{-1}$$

$$\alpha_{CCT}^{failure} = \alpha_{max,CCT} - 1.96\frac{\sigma}{\sqrt{N}} \quad (8)$$
$$= -3.01\,x10^{-6}\ hour^{-1}$$

Where $\alpha_{LM}^{failure}$ is the failure threshold of the decay rate for the normalized luminous flux output, and $\alpha_{CCT}^{failure}$ is the failure threshold of the decay rate for the normalized correlated color temperature.

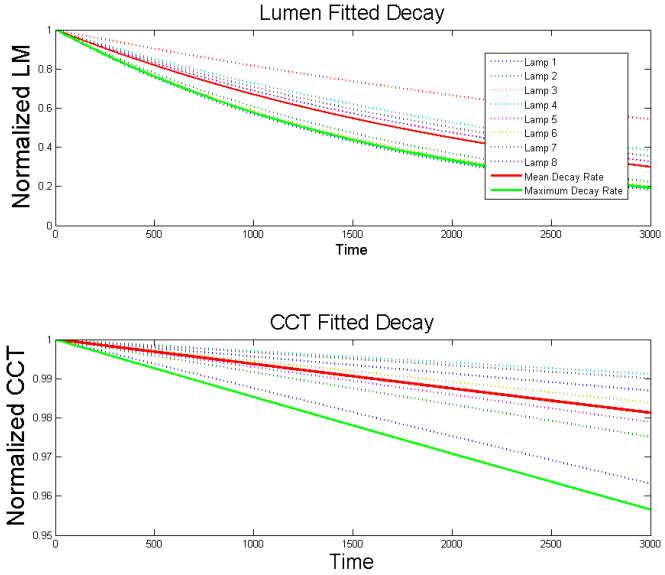

Figure 8: Characterized Decay Rate Curve for the LED Lamp

The decay rate values from the LUXEON LEDs have been used to compute the LED related decay rate for the lamp. The failure threshold decay rate has been calculated using an Arrhenius model:

$$L\alpha_{LM}^{failure} = \alpha_{LM}^{failure} \cdot e^{-\frac{E_A}{K_B}\left(\frac{1}{T_1}-\frac{1}{T_2}\right)} \quad (9)$$
$$= -5.55\,x\,10^{-4}\ hour^{-1}$$

$$L\alpha_{CCT}^{failure} = \alpha_{CCT}^{failure} \cdot e^{-\frac{E_{act}}{k_B}\left(\frac{1}{T_1}-\frac{1}{T_2}\right)} \quad (10)$$
$$= -1.48\,x10^{-5}\ hours^{-1}$$

The time dependent decay curve for the LED Lamp is shown in Figure 8a where the bold red line is the mean decay rate. The lower-bound is depicted as a green line in a Figure 8a. The CCT decays almost linearly. However, the Lumen Maintenance exhibits much more exponential pattern. The green dash line in Figure 10b shows the failure criterion for the LED Lamp. Figure 8b shows that all of CCT degradation lines are higher than the failure threshold. Only one of the tested samples lies on the failure threshold for Lumen Maintenance.

VI. Bayesian Probabilistic Model

In this paper, Bayesian Probabilistic Generative Models [Bishop 2006] have been used to classify and separate damaged solid state luminaire assemblies from healthy assemblies. The goal of classification is to analyze input vector, x consisting of CCT, Color-Shift and Luminous Flux Output and to assign it to one of the classes, C_k. There are two possible classes including damaged or healthy. The classes are taken to be disjoint, so that each input is assigned to only one class. The input space is divided decision regions whose boundaries are called the decision boundaries. The target variable has been represented as a binary variable such that t=1 represents class C_1 and t=0 represents class C_2. The value of 't' is the probability that the class is C_1 with the values of probability taking only extreme values of 0 and 1. The conditional probability distribution, $p(C_k \mid X)$, has been modeled in the inference stage and then the distribution has subsequently been used to make optimal decisions of classification. A generative approach has been adopted for computing the conditional probability distribution $p(C_k \mid X)$. In this procedure, the class conditional probabilities, $p(X \mid C_k)$ have been modeled as well as the class priors, $p(C_k)$, and then used to compute posterior probabilities through Bayes Theorem. For the purpose of the analysis, it was assumed that the class conditional probability density function is Gaussian, represented by:

$$P(X \mid C_k) = \frac{1}{(2\pi)^{d/2}} \cdot \frac{1}{|\Sigma_k|} \cdot \quad (11)$$
$$\exp\left(-\frac{1}{2}(X-\mu_k)^T \Sigma_k^{-1}(X-\mu_k)\right)$$

Where the input vector, x, is a d-component column vector, μ is the d-component mean vector, Σ is the d-by-d covariance matrix. The class-prior $p(C_k)$ utilizes the weighted group form, for classifying two groups, where the probabilities of each group are given by:

$$p(C_1) = \frac{N_1}{N_1+N_2}; p(C_2) = \frac{N_2}{N_1+N_2} \quad (12)$$

$$p(C_1)/p(C_2) = N_1/N_2 \quad (13)$$

Where, N_1 is the number of samples in the first group, and N is the total numbers of samples. The conditional probability distribution for classifying the 'k' group has been normalized, based on the weighted value between its posterior and the sum of posteriors from all the groups. Minimum error rate classification has been achieved through the use of discriminant functions, $p(C_k \mid X)$:

$$g_i(x) = p(C_k \mid X) = \frac{p(X \mid C_k)p(C_k)}{\sum p(X \mid C_j)p(C_j)} \quad (14)$$

Where, $g_i(x)$ is a discriminant function which is used as a classifier. Thus, the discriminant function for the multiple-class classification is defined as:

$$g_i(x) = p(X \mid C_k)p(C_k) \quad (15)$$

Alternatively, the discriminant may be represented in log-form as,

$$g_i(x) = \ln p(X \mid C_k) + \ln p(C_k) \quad (16)$$

In a general multivariate normal case, the covariance matrices are different for each category. The discriminant function can be computed by substituting Equation (11) for the class conditional probability density function into Equation (16) for the long-form of the discriminant function as follows:

$$g_i(x) = -\frac{1}{2}(x-\mu_i)^T \Sigma_i^{-1}(x-\mu_i) - \frac{d}{2}\ln 2\pi - \frac{1}{2}\ln|\Sigma_i| + \ln p(\quad (17)$$

Where the input vector, x, is a d-component column vector, μ is the d-component mean vector, Σ is the d-by-d covariance matrix. The resulting discriminant terms are inherently quadratic:

$$g_i(x) = X^T.W_i \cdot X + w_i^T \cdot X + \omega_{i0} \quad (18)$$

Where the quadratic coefficients are solved as:

$$W_i = -\frac{1}{2}\left(\Sigma_i^{-1}\right) \quad (19)$$

$$w_i = \left(\Sigma_i^{-1} \cdot \mu_i\right) \quad (20)$$

$$w_{i0} = -\frac{1}{2}\left(\mu_i^T \Sigma_i^{-1} \mu_i\right) - \frac{1}{2}\left(\ln|\Sigma_i|\right) + \ln p(C_k) \quad (21)$$

The discriminant functions have been computed for all the samples and the samples assigned to the class corresponding to the highest discriminant. The decision boundaries have been computed by setting

$$g_1(x) = g_2(x) \quad (22)$$

VII. Feature Space Creation

A two dimensional feature space has been created for classification of the test data. The two dimensions include the normalized luminous flux output and the correlated color temperature. The decay rate failure thresholds for the solid state luminaires which have been computed previously (Equations (9) and (10)) are used to construct the failure boundary for luminous flux output and a second boundary for the correlated color temperature. Lamps could fail because they breach the failure boundary for either the luminous flux output, correlated color temperature or both. The time at which the lamp breaches either boundary is termed as the failure time and represented by T_{CF}. The luminous flux output and the correlated color temperature at the failure boundary for failure time (T_{CF}) has been computed based on the previously calculated maximum decay rate.

$$\Phi = \beta \cdot e^{\alpha \cdot t} \quad (23)$$

$$LM_{max\ failure} = (100) \cdot e^{L\alpha_{LM}^{failure} \cdot T_{CF}} \quad (24)$$

$$CCT_{max\ failure} = (100) \cdot e^{L\alpha_{CCT}^{failure} \cdot T_{CF}} \quad (25)$$

Where the multiplier of '100' in Equations (24) and (25) was used to change the computed normalized values into percentages.

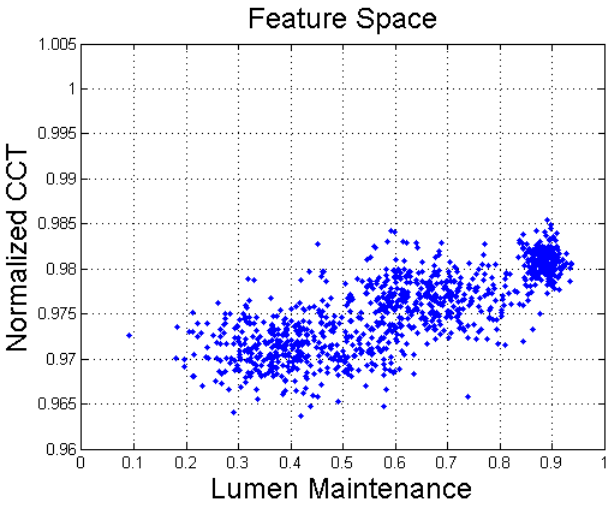

Figure 9: Feature space containing data of lamp's current state, lamp's failure threshold, and pristine healthy distribution of lamps prior to classification.

The computed locations in the feature space allow the location of the failure threshold versus the current state of the lamp in the feature space. The mean and variance of the failure threshold and location at the failure time has been computed for all the devices under test. The classification of the healthy lamps versus the damaged lamps was accomplished using a decision boundary computed based on the discriminant function (Equation (18)). The test lamps have been classified as belonging to the failure threshold distribution or the healthy distribution. The correlation between the luminous flux output and the correlated color temperature has been removed by computing the principal directions of the variance to yield uncorrelated x-axis and y-axis variances. The covariance matrix for the 85C/85%RH dataset is presented by,

$$\Sigma = \begin{pmatrix} \Sigma_{aa} & \Sigma_{ab} \\ \Sigma_{ba} & \Sigma_{bb} \end{pmatrix} \quad (26)$$

The covariance matrix has been decorrelated by computing the principal components, thus rendering the correlation matrix in the form,

$$\Sigma = \begin{pmatrix} \Sigma_{11} & 0 \\ 0 & \Sigma_{22} \end{pmatrix} \quad (27)$$

Where the subscripts '1' and '2' indicate the principal directions. The distributions of the lamp-state and the lamp's failure threshold have been transformed into the decorrelated principal component feature space for the purpose of classification. The data groups plotted in Figure 9 include the lamp's current state, lamp's failure threshold, and the pristine healthy distribution of lamps prior to classification.

VIII. Bayesian Regression Model

The response variables of luminous flux output, and CCT are the target variables (t) for the Bayesian regression models. Input parameters (w) include weights for the input parameters of time. The posterior probability has been computed based on the conditional probability:

$$p(t \mid w) = \frac{p(w \mid t)p(t)}{P(w)} \quad (28)$$

Where, $p(t \mid w)$ is the normalized conditional posterior of the target variables, and $p(t)$ is the prior distribution of the target variables. The Bayesian conjugate prior Gaussian probability is represented as follows:

$$P(W) = N(W \mid M_0, S_0) = N(W \mid 0, \alpha^{-1}I) \quad (29)$$

Where, α is the precision parameter of the weight distribution. The real-valued input variable column vector is:

$$X = [x_1 \quad x_2 \quad \ldots \quad x_n]^T \quad (30)$$

The real-valued predict target column vector is represented as,

$$T = [t_1 \quad t_2 \quad \ldots \quad t_n]^T \quad (31)$$

Candidate basis functions used may include polynomial functions (ϕ) with weights (w). The basis function 1×M matrix can be shown as the following:

$$\Phi(x) = [1 \quad x \quad x^2 \quad \ldots \quad x^M]^T \quad (32)$$

The weights M×1 matrix is represented as:

$$W = \begin{bmatrix} w_0 \\ w_1 \\ w_2 \\ \ldots \\ w_M \end{bmatrix} \quad (33)$$

The future degradation of the luminaire can be calculated from the estimation matrix as follows:

$$t_i = W^T \cdot \Phi(x_i) \quad (34)$$

The likelihood function will be represented with a Gaussian probability distribution as follows,

$$P(t \mid x, W, \beta) = N(t \mid W^T \cdot \Phi(x_i), \beta^{-1}I) \quad (35)$$

Where W is the weight vector and β is the precision of the target variable distribution, t. The n- set of observations $t_1, \ldots, t_N$, have been combined into a matrix T of size N × K such that the nth row is given by t_{Tn} . Similarly, we can combine the input vectors $x_1, \ldots, x_N$ into a matrix X. The log-likelihood of the data-set is given by:

$$\ln P(T \mid X, W, \beta) = \sum_{n=1}^{N} \ln N(t \mid W^T \cdot \Phi(x_i), \beta^{-1}I) \quad (36)$$

The likelihood represented by Equation (36) that the target, t corresponds to the input variable sets being considered is maximized with respect to β. The target parameter's variance is represented by:

$$\frac{1}{\beta_{ML}} = \frac{1}{N}\sum_{i=1}^{N}(y_i - t_i)^2 = \frac{1}{N} \cdot (Y - T) \cdot (Y - T)^T \quad (37)$$

The variance computed from equation (37) corresponds to the maximum value of the likelihood function. We can substitute the β_{ML} into Equation (36) for $P(T \mid X, W, \beta)$, which gives:

$$P(T \mid X, W, \beta) = \prod_{i=1}^{n} N(t \mid W^T \cdot \Phi(x_i), \beta_{ML}^{-1}) \quad (38)$$

The weight vector will be updated using the Bayesian posterior conditional probability represented as follows:

$$P(W \mid X, T, \alpha, \beta) \propto P(T \mid X, W, \beta) \cdot P(W \mid \alpha) \quad (39)$$

$$= N(W \mid M_N, S_N)$$

$$M_N = S_N(S_0^{-1}M_0 + \beta\Phi^T T)$$

$$S_N^{-1} = S_0^{-1} + \beta\Phi^T\Phi$$

Where, M_N is the mean and S_N is the covariance of the Bayesian posterior conditional probability

$$M_N = S_N(S_0^{-1}M_0 + \beta\Phi^T T) \quad (40)$$

$$S_N^{-1} = S_0^{-1} + \beta\Phi^T\Phi$$

The prediction of the target vector at the next time step is represented as:

$$P(t \mid T, \alpha, \beta) = \int P(t \mid W, \beta) \cdot P(W \mid T, \alpha, \beta) dW \quad (41)$$

The condition distribution $P(t \mid T, \alpha, \beta)$ has been calculated out as the distribution and probability with its mean and variance depending on the variable 'x'; Therefore, we can finally predict each output 't' including luminous flux and correlated color temperature from each time series input 'x', such as:

$$P(t \mid x, T, \alpha, \beta) = \quad (42)$$

$$N(t \mid M_N^T\Phi(x), \beta^{-1} + \Phi^T(x)S_N\Phi(x))$$

IX. Failure Analysis Results

Once the Bayesian classifier has finished the training process, the data mapped onto the feature space is classified. The discriminant function has been used to classify the samples in the feature space and formulate a decision boundary between the lamps with accrued damage and pristine samples. The lamps migrate in the feature space from the top right to the bottom left with the increase in the amount of accrued damage. In Figure 10, the red data points are the healthy samples and the green data points are the samples with accrued damage. The red dash line shows the failure threshold between the healthy lamps and lamps with accrued damage. The decision boundary has been calculated such that the discriminant for the two classes has an equal value along the boundary.

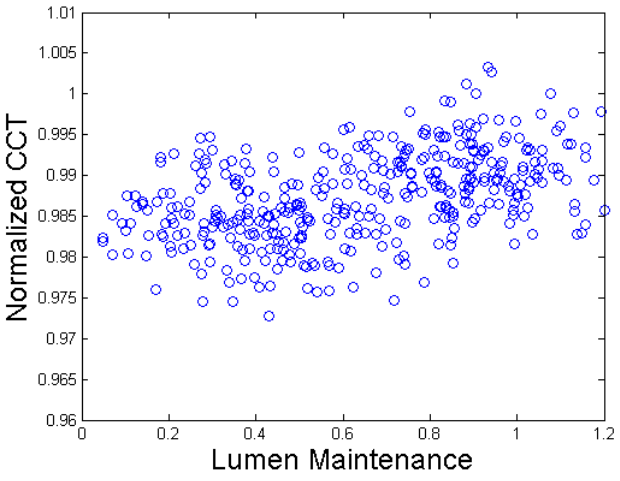

(a)

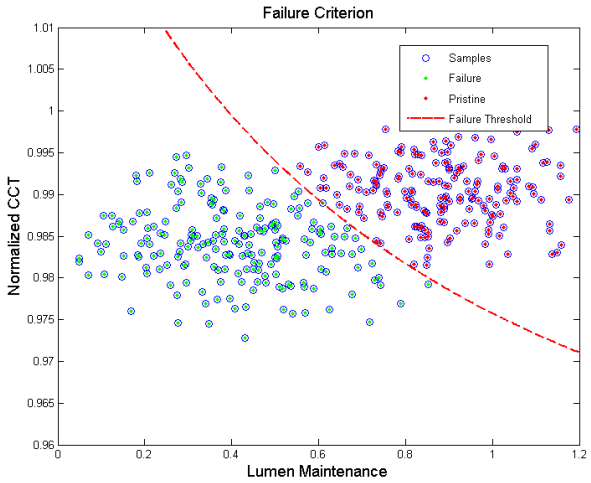

(b)

Figure 10: (a) End of Life distribution and pristine for LED Lamp (b) Failure Criterion for Distribution Classification. LEGEND: The red dash line shows the failure threshold between the healthy lamps and lamps with accrued damage; red data points are the healthy samples and the green data points are the samples with accrued damage.

The values of the coefficients of the polynomial that describes the decision boundary have been calculated using the following equations,

$$F(x,y) = I^T W_2 I + W_1^T I + W_0 \quad (43)$$

$$I = \begin{bmatrix} x \\ y \end{bmatrix} \quad (44)$$

$$W_2 = -\frac{1}{2}\Sigma_i^{-1} \quad (45)$$

$$W_1 = \Sigma_i^{-1}\mu_i$$

$$W_0 = -\frac{1}{2}\mu_i^T\Sigma_i^{-1}\mu_i - \frac{1}{2}\log|\Sigma_i| + \log(p(C_i))$$

The matrix expression of $F(x,y)$ has been expanded as the quadratic area function:

$$F(x,y) = W_2(1,1)x^2 + 2W_2(1,2)xy + W_2(2,2)y^2 \quad (46)$$
$$+ W_1(1,1)x + W_1(2,1)y + W_0$$

The classification decision boundary for the failure threshold can be calculated from previous analysis as equating the PDFs for the classes on either side of the decision boundary:

$$G(x,y) = F_1(x,y) - F_2(x,y) = 0 \quad (47)$$
$$= 3.72x^2 - 157.74xy + 131.11x +$$
$$1823.78y^2 - 3984.71y + 2170.75$$

From the classification, the calculated coefficients of the polynomial are:

$$W0 = -2.7019 \cdot 10^4 \quad (48)$$

$$W1 = \begin{bmatrix} 0.0305 \\ 5.4802 \end{bmatrix} \cdot 10^4 \quad (49)$$

$$W2 = \begin{bmatrix} -0.0016 & -0.0149 \\ -0.0149 & -2.7783 \end{bmatrix} \cdot 10^4 \quad (50)$$

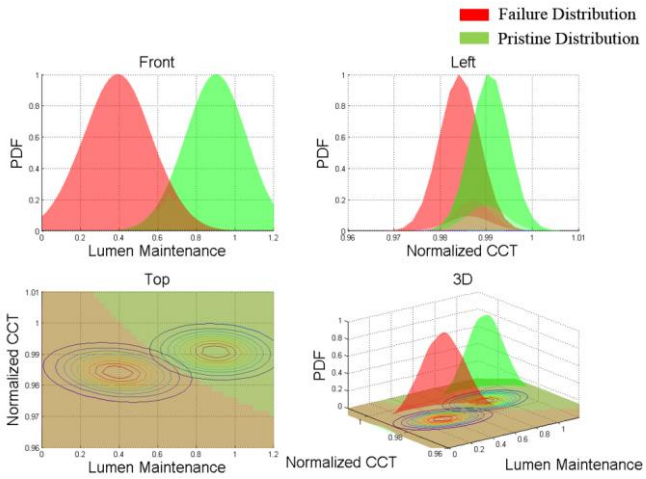

Figure 11: Classification of the lamps with accrued damage and pristine lamp PDFs. LEGEND: red PDF is corresponding to the lamps with accrued damage while the green PDF are the healthy lamps

Overall, the Bayesian unsupervised classifier is powerful classification tool. Even though two groups have been classified, the technique presented is applicable to multiple groups. The distributions corresponding to the healthy group with significant accrued damage has been plotted. The red PDF is corresponding to the lamps with accrued damage while the green PDF are the healthy lamps. The overlapping area displays the transition failure area between the healthy and the lamps with accrued damage. Typically, we want this overlapping PDF region to be as small as possible. The decision boundary has been updated as more data becomes available for the different classes. Figure 12 shows the three groups classification, which we assign the initial parametric distributions for the (a) failure threshold (b) the pristine LED Lamp group and (c) damaged LED Lamp group. The testing data has been grouped, and Bayesian Classifier calculates the mean and variance numerically.

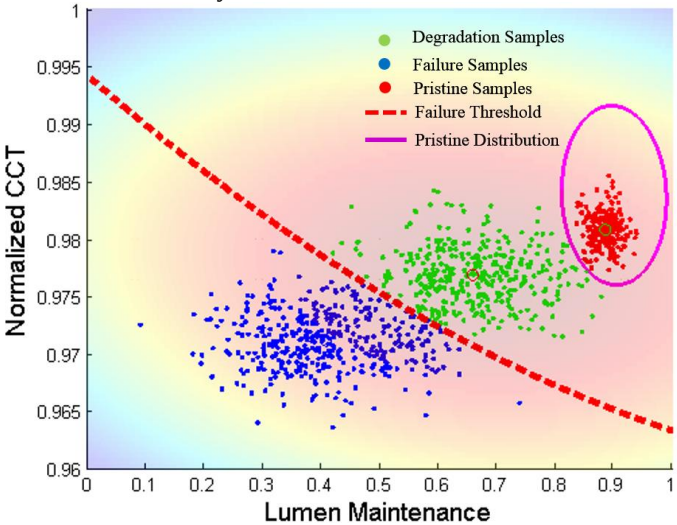

Figure 12: L70 Time Decision Boundary. LEGEND: RED dots – pristine LEDs; GREEN dots – LEDs with

significant accrued damage; BLUE dots – failed LEDs in which the lumen flux degradation has dropped below 70-percent of the initial luminous flux output in nearly all the tested samples.

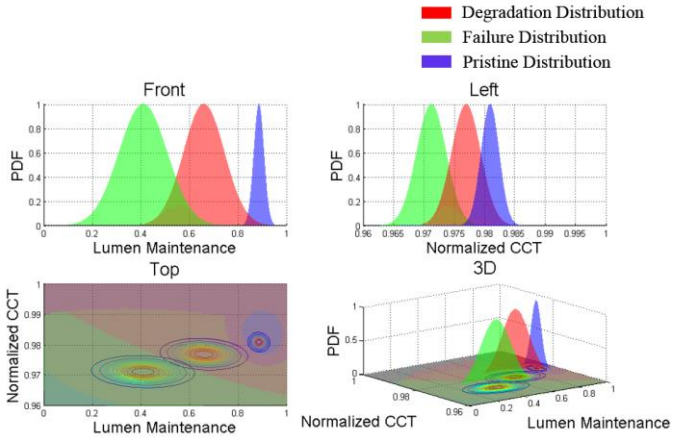

Figure 13: Critical Failure, LED Lamp Failure and Pristine Lamp PDF Distribution. LEGEND: BLUE– pristine LEDs; RED– LEDs with significant accrued damage; GREEN– failed LEDs in which the lumen flux degradation has dropped below 70-percent of the initial luminous flux output in nearly all the tested samples.

Figure 12 shows the migration of decision boundary. The decision boundary between pristine lamp group and failure lamp group is shown with a solid magenta ellipse, and the decision boundary between the failure threshold and the lamps with accrued damage is shown with a dashed red line. The Figure 13 demonstrates the three PDFs for the pristine LED Lamp, damaged lamp group as well as lamp group beyond the failure threshold. The decision boundary between the damaged lamp group and the group beyond the failure threshold has been termed as the critical failure boundary, which should not be breached to avoid failure.

X. Remaining Useful Life

Bayesian regression method has been used to determine the Remaining Useful Life (RUL) for every test lamp. Lumen Maintenance (LM) degradation has been used as the main indicator of system decay, by fitting the Lumen Maintenance degradation curve (Figure 14). Figure 15 shows the training of the Bayesian regression model through the maximum likelihood function and prediction of the posterior distributions. The process discussed previously in the Bayesian regression section, has been used for the future state prediction of the lamp's luminous flux and the remaining useful life. Figure 16 shows the Bayesian linear regression for the third order polynomial model with four weights. The green dots are the measured data points, and the red dots show the predicting decay curve. The testing length is up to 2537 hours. The Remaining Useful Life (RUL) has been calculated by predicting the future luminous flux output state till the L70 threshold.

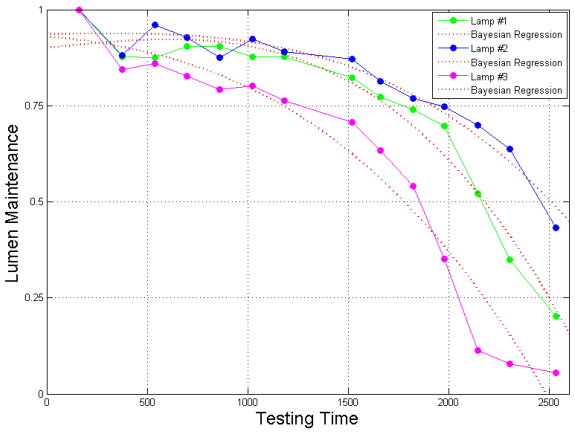

Figure 14: Lumen Maintenance Regression for LED Lamp

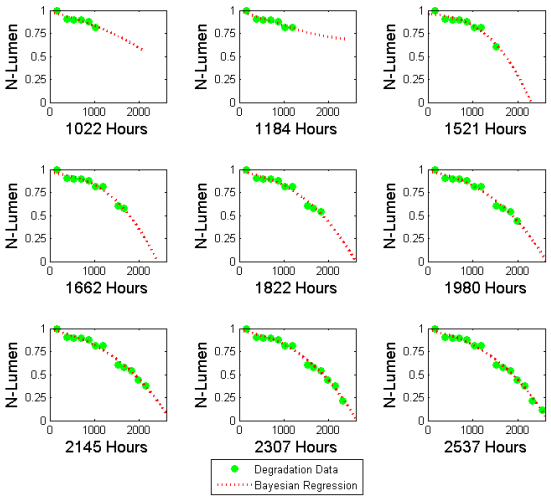

Figure 15: Bayesian Regression Learning Process. LEGEND: GREEN dots are the actual measured data; RED lines are the model prediction of the lumen flux output using Bayesian Regression.

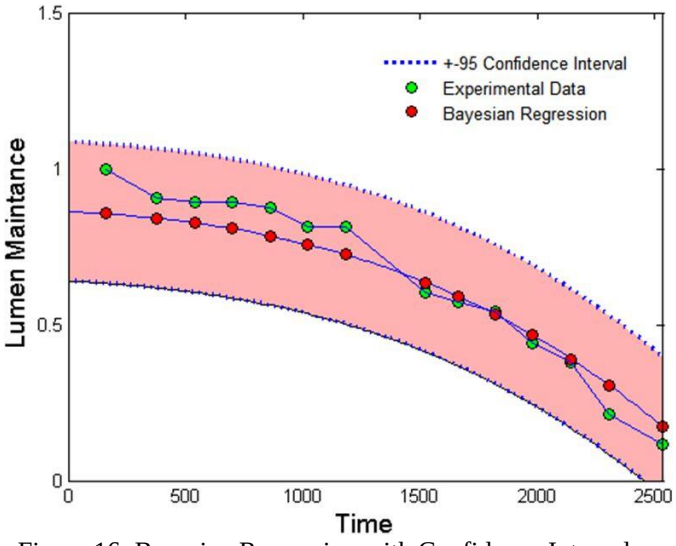

Figure 16: Bayesian Regression with Confidence Interval

The predicted RUL is known as the predicted End of Life (EoL) minus the sampling time, represented by:

$$T_{predict} = P_{EoL} - T_{sample} \quad (51)$$

The real RUL is known as the actual EoL minus the sampling time. So the algebra equation presents as following:

$$T_{actual} = A_{EoL} - T_{sample} \quad (52)$$

A two parameter weibull distribution has been used to model the lamp failures. The probability density function for the two parameter Weibull distribution has the following form:

$$f(t) = \frac{\beta}{\eta}\left(\frac{t}{\eta}\right)^{\beta-1} e^{-\left(\frac{t}{\eta}\right)^{\beta}} \quad (53)$$

Where β is the shape parameter, η is the characteristic life. The estimated shape parameter and the characteristic life are: $\beta = 7.1$ and $\eta = 1790$ hours. Since the $\beta > 1.0$, it indicates that the failures are wear out failures. The Weibull cumulative distribution, the population fraction failing by time t is given as following CDF:

$$F(t) = 1 - e^{-(t/\eta)^{\beta}} = 1 - e^{-(t/1790.1)^{7.1}} \quad (54)$$

The reliability function is thereby given by the 1-F(t). The CDF indicates that once time reached 1700.2 hours the LED lamp reliability dropped to 50%. The characteristic life (B63.2 life) is 1790.1 hours, which says 63.2% LED lamps have failed at this time in the accelerated test condition of 85℃/85%RH.

$$R(t) = 1 - F(t) = e^{-(t/\eta)^{\beta}} = e^{-(t/1790.1)^{7.1}} \quad (55)$$

Figure 17 shows the representative samples of the failed lamps with and without the lens. Note that encapsulant of several of the LEDs in the failed lamps shows distinct discoloration. It is hypothesized that the discoloration of the encapsulant was a major contributor to the degradation in the luminous flux output and the color shift during the 85C/85%RH accelerated test.

Figure 17 Representative Samples of the Failed Lamps with and without the Lens.

XI. Summary and Conclusions

The 60W LED lamps have been studied under the accelerated test conditions of 85℃/85%RH for both luminous flux output and the correlated color temperature. A Bayesian framework for early classification of the failed lamps in the luminous flux and correlated color temperature feature space has been formulated and demonstrated on the test-population of the lamps. Failures have been identified because of problems of luminous flux degradation or color shift or both. In addition the Bayesian regression model has been developed to predict the luminous flux degradation till the L70 threshold widely used as definition of failure for the solid state luminaires. The proposed methodology allows the early identification of the onset of failure much prior to development of complete failure distributions and can be used for assessing the damage state of SSLs in fairly large deployments. The α-λ plots have been used to evaluate the robustness of the proposed methodology. Results show that the predicted degradation for the lamps tracks the true degradation observed during 85℃/85%RH during accelerated life test fairly closely within the ±20% confidence bounds. Failure modes of the test population of the lamps have been studied to understand the failure mechanisms in 85℃/85%RH accelerated test. Results indicate that the dominant failure mechanism is the discoloration of the LED encapsulant inside the lamps which is the likely cause for the luminous flux degradation and the color shift.

Acknowledgments

The work presented here in this paper has been supported by a research grant from the Department of Energy under Award Number DE-EE0005124.

References

[1]. Baillot, R., Deshayes, Y., Bechou, L., Buffeteau, T., Pianet, L., Armand, C., Voillot, F., Sorieul, S., Ousten, Y. "Effects of Silicone Coating Degradation on GaN MQW LEDs Performances Using Physical and Chemical Analysis." *Microelectronics Reliability* 50(2010): 1568-1573.

[2]. Bishop, C. M., Pattern Recognition and Machine Learning, Springer Science-Business Media, LLC, 2006.

[3]. Byung-Lip Ahn, Cheol-Yong Jang, Seung-Bok Leigh, Seunghwan Yoo, Hakgeun Jeong, Effect of LED Lighting on Cooling and Heating Load in Buildings, Applied Energy, Volume 113, Pages 1484–1489,

January 2014.
[4]. Chan, S.I., W.S. Hong, K.T. Kim, Y.G. Yoon, J.H. Han, J.S. Jang, Accelerated life test of high power white light emitting diodes based on package failure mechanisms, Microelectronics Reliability 51 (2011) 1806–1809.
[5]. Choi, M., Ki Hyun Kim, Changhun Yun, Dai Hyoung Koo, Sang Bin Song, Jae Pil Kim, Direct correlation between reliability and pH changes of phosphors for white light-emitting diodes, Microelectronics Reliability 54 (2014) 2849–2852.
[6]. Cree. "Cree Xlamp XR Family LED Reliability, CLD-AP06 Rev. 7." Cree Inc. 2009.
[7]. Duda, R.O., Peter E. Hart, David G. Stork. Pattern Classification, Second Edition, Wiley & Sons, ISBN: 978-0-471-05669-0, 2001
[8]. Fu, Han-Kuei, Chin-Wei Lin, Tzung-Te Chen, Chiu-Ling Chen, Pei-Ting Chou, Chien-Jen Sun, Investigation of dynamic color deviation mechanisms of high power light-emitting diode, Microelectronics Reliability 52 (2012) 866–871.
[9]. Hewlett Packard. "Reliability of Precision Optical Performance AllnGaP LED Lamps in Traffic Signals and Variable Message Signs." *Application Brief I-004* (1997)
[10]. Hsu, Y., Lin, Y., Chen, M., Tsai, C., Kuang, J., Huang, S., Hu, H., Su, Y. and Cheng, W. "Failure Mechanisms Associated with Lens Shape of High-Power LED Modules in Aging Test." *IEEE Trans. on Electron Devices* 55(2008): 689-694.
[11]. IES (Illuminating Engineering Society), IES LM-80-08. "Approved Method: Measuring Lumen Maintenance of LED Light Sources." 2008
[12]. IES (Illuminating Engineering Society), IES TM-21-11. "Projecting Long Term Lumen Maintenance of LED Light Sources" 2008
[13]. Jang, Daeseok, Se-Jin Yook, Kwan-Soo Lee, Optimum design of a radial heat sink with a fin-height profile for high-power LED lighting applications, Applied Energy, Volume 116, 1, Pages 260–268, March 2014
[14]. Lall, P., Sakalaukus, P., Davis, L., Prognostics of Damage Accrual in SSL Luminaires and Drivers Subjected to HTSL Accelerated Aging, Proceedings of the ASME 2013 International Technical Conference & Exposition on Packaging and Integration of Electronic and Photonic Microsystems, InterPACK2013-73250, pp. 1-8, Burlingame, CA, 2013.
[15]. Lall, P., Wei, J., & Davis, L., Prediction of L70 lumen maintenance and chromaticity for LEDs using extended Kalman filter models, SPIE Optical Engineering+ Applications (pp. 88350M-88350M-19), San Diego, CA, 2013.
[16]. Lall, P., Wei, J., Davis, L., L70 Life Prediction for Solid State Lighting Using Kalman Filter and Extended Kalman Filter Based Models, Electronic Components and Technology Conference, ECTC, 63rd, pp.1452-1465, 2013.
[17]. Lall, P., Wei, J., Davis, L., Solid State Lighting Life Prediction Using Extended Kalman Filter, Proceedings of the ASME 2013 International Technical Conference & Exposition on Packaging and Integration of Electronic and Photonic Microsystems, InterPACK2013-73288, pp. 1-11, Burlingame, CA, 2013.
[18]. Lall, P., Zhang, H., Davis, L., Assessment of Lumen Degradation and Remaining Life of LEDs using Particle Filter, Proceedings of the ASME 2013 International Technical Conference & Exposition on Packaging and Integration of Electronic and Photonic Microsystems, InterPACK2013-73305, pp. 1-13, Burlingame, CA, 2013.
[19]. Lumileds. "Luxeon Reliability." *Philips Lumileds Reliability Datasheet RD25* (2006).
[20]. Luo, X., Wu, B. and Liu, S. "Effects of Moist Environments on LED Module Reliability." *IEEE Trans. on Device and Materials Reliability* 10(2010): 182-186.
[21]. Meneghini, M., M. Dal Lago, L. Rodighiero, N. Trivellin, E. Zanoni, G. Meneghesso, Reliability issues in GaN-based light-emitting diodes: Effect of dc and PWM stress, Microelectronics Reliability 52 (2012) 1621–1626.
[22]. Meneghini, M., Trevisanello, L., Meneghesso, G. and Zanoni, E. "A Review on the Reliability of GaN-Based LEDs." *IEEE Trans. on Device and Materials Reliability* 8(2008): 323-331.
[23]. Narendran, N., Gu, Y., Freyssinier, J.P., Yu, H. and Deng, L. "Solid-State Lighting: Failure Analysis of White LEDs." *Journal of Crystal Growth* 268(2004): 449-456.
[24]. Nichia. "Specifications for Nichia Chip Type White LED Model: NCSW119T-H3. Nichia STS-DA1-0990A." Nichia Corp. 2009
[25]. Sawyer, S., Rumyantsev, S., & Shur, M. (2008). Degradation of AlGaN-based ultraviolet light emitting diodes. Solid-State Electronics, Elsevier, Pages 968-972.
[26]. Saxena, A., Celaya, J., Saha, B., Goebel, K., Evaluating algorithm performance metrics tailored for prognostics. IEEE Aerospace conference, 2009[a].
[27]. Saxena, A., Celaya, J., Saha, B., Saha, S., Goebel, K., On Applying the Prognostics Performance Metrics, Annual Conference of the PHM Society, vol 1, San Diego, CA, 2009[b].
[28]. Saxena, A., J. Celaya, B. Saha, S. Saha, and K. Goebel, Evaluating Algorithm Performance Metrics Tailored for Prognostics, IEEE Aerospace Conference, Big Sky, MT, pp. 1-11, March 2008[a].
[29]. Saxena, A., J. Celaya, E. Balaban, K. Goebel, B. Saha, S Saha, and M. Schwabacher, Metrics for Evaluating Performance of Prognostic Techniques, Intl. Conf. on Prognostics and Health Management, Denver, Colorado, pp. 1-17, October 2008[b].
[30]. US Energy Information Administration, Retrieved from U.S Energy Information Administration, Page accessed June 27, 2014, http://www.eia.gov/tools/faqs/faq.cfm?id=99&t=3, 2012
[31]. Wang, F.-K. (2012). Lifetime predictions of LED-based light bars by accelerated degradation test.

Microelectronics Reliability, Elsevier, Pages 1332-1336.

[32]. Yang, Shih-Chun, Pang Lin, Chien-Ping Wang, Sheng Bang Huang, Chiu-Ling Chen, Pei-Fang Chiang, An-Tse Lee, Mu-Tao Chu, Failure and degradation mechanisms of high-power white light emitting diodes, Microelectronics Reliability 50 (2010) 959–964.

AUTHOR BIOGRAPHY

Pradeep Lall (M'93—SM'08—F'12) is the Thomas Walter Professor with the Department of Mechanical Engineering, and the Director of the NSF Center for Advanced Vehicle and Extreme Environment Electronics at Auburn University. He received the B.E. degree in mechanical engineering from the Delhi College of Engineering, Delhi, India, in 1988, the M.S. and Ph.D. degrees in mechanical engineering from the University of Maryland, College Park, in 1989 and 1993, respectively, and the M.B.A. degree from Kellogg School of Management, Northwestern University, Evanston, IL, in 2002. He was previously with Motorola's Wireless Technology Center. He has published extensively in the area of electronic packaging with emphasis on modeling and predictive techniques. He is author and co-author of 2-books, 14 book chapters, and over 400 journal and conference papers in the field of electronic packaging with emphasis on design, modeling, and predictive techniques. Dr. Lall is Fellow of the IEEE, a Fellow of the ASME, and a Fellow of the Alabama Academy of Science. Dr. Lall is the recipient of the IEEE Exceptional Technical Achievement Award, ASME's Applied Mechanics Award, SMTA's Member of Technical Distinction Award, Auburn University's Creative Research and Scholarship Award, SEC Faculty Achievement Award, Samuel Ginn College of Engineering Senior Faculty Research Award, Three-Motorola Outstanding Innovation Awards, Five-Motorola Engineering Awards, and Twenty Best-Paper Awards at national and international conferences. He holds three U.S. Patents. Dr. Lall has served in several distinguished roles at national and international level including serving as member of National Academies Committee on Electronic Vehicle Controls, Member of the IEEE Reliability Society AdCom, IEEE Reliability Society Representative on the IEEE-USA Government Relations Council for R&D Policy, Chair of Congress Steering Committee for the ASME Congress, Member of the technical committee of the European Simulation Conference EuroSIME, and Associate Editor for the IEEE Transactions on Components and Packaging Technologies. He is a Six-Sigma Black-Belt in Statistics. He is the founding faculty advisor for the SMTA student chapter at Auburn University, and a member of the editorial advisory board for SMTA Journal.

Junchao Wei received the B.E., degree from Hunan University of Technology, Zhuzhou, China, in 2011. Currently, he is Ph.D. student in Mechanical Engineering at Auburn University, and works as a research assistant for the CAVE3 (The NSF Center for Advanced Vehicle and Extreme Environment Electronics). His research areas include LED Reliability models, X-ray CT scan detection and three dimensional reconstruction; deformation and strain measurement; electronics reliability and prognostics; algorithm development; computational models for reliability of thermal, shock, drop, and vibration.

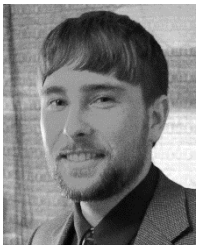

Peter J. Sakalaukus, Jr. (M'12) received the B.S. degree in mechanical engineering from Mississippi State University, Starkville, MS, in 2006 and the M.S. degree in mechanical engineering from the University of South Alabama, Mobile, AL, in 2011. He is currently pursuing the Ph.D. degree in mechanical engineering at Auburn University, Auburn, AL.